Journal of Environmental Chemical Engineering 11 (2023) 110639

Contents lists available at ScienceDirect

Journal of Environmental Chemical Engineering

journal homepage: www.elsevier.com/locate/jece

What is the most effective percentage of Rose Bengal on polyamide fabrics for the visible-light photoinactivation of Gram-positive bacteria?

Jenny Flores [a,1], Alberto Blázquez-Moraleja [a,b,1], Marilés Bonet-Aracil [c], Pilar Moya [d], Francisco Bosca [a,*], M. Luisa Marin [a,*]

[a] Instituto Mixto de Tecnología Química, Universitat Politècnica de València-Consejo Superior de Investigaciones Científicas, Avda. de los Naranjos s/n, Valencia E-46022, Spain
[b] Universidad Complutense de Madrid, Ciudad Universitaria s/n, E-28040 Madrid, Spain
[c] Departamento de Ingeniería Textil y Papelera, Universitat Politècnica de València, Plaza Ferrándiz y Carbonell s/n, 03801 Alcoy, Spain
[d] Centro Ecología Química Agrícola, Instituto Agroforestal Mediterráneo, Universitat Politècnica de València, Avda Naranjos s/n, Valencia E-46022, Spain

ARTICLE INFO

Editor: Despo Fatta-Kassinos

Keywords:
Photodynamic inactivation
Photophysical properties
Photosensitizer
Reactive oxygen species

ABSTRACT

Heterogeneous photocatalysts based on fabric materials have achieved great relevance for water disinfection. However, studies have yet to be performed looking for the best percentage of a photosensitizer on fabric, considering the $^1O_2$ generation efficiency as well as the charge distribution of the dye fabrics surface for bacterial inactivation. Therefore, polyamide fabrics (PAF) dyed at different Rose Bengal (RB) percentages (RB-PAF) as an anionic photosensitizer were prepared to determine the best value for photodynamic inactivation of Gram-positive bacteria (*Enterococcus faecalis*). Time-resolved and steady-state emission measurements, as well as laser flash photolysis experiments, were also performed. RB-PAF at a percentage of 1% (on-weigth-of-fiber, o.w.f.) showed 100% inactivation efficiency against *E. faecalis* (reduction of more than 6 $\log_{10}$ units in the viable count) in only 15 min. Contrarily, fabrics with RB values of 0.5 or 3% (o.w.f.) showed no bacterial inactivation or only a small activity (1 $\log_{10}$ unit reduction), respectively. Results revealed that the effects observed by RB-PAF are mediated by ^{3}RF* and the subsequent generation of $^1O_2$. The insignificant photooxygenation of 9,10-dimethyl anthracene observed for RB-PAF at 0.5% explains the lack of bacterial inactivation, while the low effect observed for RB-PAF at 3% is produced by electrostatic repulsions between the anionic RB and the bacteria surface. These results reveal that in order to design newly dyed fabrics for disinfection, it is important to optimize the percentage of dye to avoid aggregation of photosensitizers and to obtain an adequate net negative charge distribution in the antimicrobial fabrics.

1. Introduction

Microbiological contamination of water sources still represents one of the main sanitary problems worldwide, with over 2 billion people not having access to clean drinking water [1]. Exposure to contaminated drinking water is one of the main causes of death in Europe and the second one worldwide, with approximately 17 million deaths annually. The main pathogenic microorganisms are reported to be *Enterococcus faecalis*, *Staphylococcus aureus*, *Klebsiella, Acinetobacter*, *Pseudomonas aeruginosa,* and *Escherichia coli* [2,3], and they are mainly spread by human and animal wastes [4]. The importance of water disinfection has been considered a worldwide concern, mainly related to the protection of the environment and human health [5]. The lack of adequate wastewater treatment facilities in developing countries represents a very serious health hazard, but also the improper management of urban and industrial wastewater often results in the inefficient removal of such pathogenic microorganisms. That is why new strategies are being sought to develop efficient and innovative methods for the disinfection of wastewater.

Recently, advanced oxidation processes (AOPs) involving heterogeneous photocatalysts have gained attention over traditional processes due to their simplicity and quick oxidation of pollutants and bacteria in water [6]. In addition, the heterogeneous photocatalysis process for water treatment presents numerous advantages, such as the dispersion

* Corresponding authors.
E-mail addresses: fbosca@itq.upv.es (F. Bosca), marmarin@qim.upv.es (M.L. Marin).
[1] These authors have contributed equally to this work

https://doi.org/10.1016/j.jece.2023.110639
Received 31 May 2023; Received in revised form 18 July 2023; Accepted 25 July 2023
Available online 27 July 2023

or suspension of the photocatalytic materials facilitating their subsequent recovery after the disinfection/decontamination process [7–10]. In particular, there is great interest in the use of organic photosensitizers, such as dyes, because they can be excited by solar energy and generate oxidative species that can react with proteins, lipids, and nucleic acids of microorganisms. As a consequence, disruption of the cell wall, alteration of the functionality of macromolecules, or inhibition of their metabolism through type I (electron transfer) and type II (singlet oxygen reaction) photoinactivation mechanisms are caused [11–15]. Their multiple advantages have led to numerous studies on the application of photochemical processes for the inactivation of bacteria [16–18]. Heterogenization of the photosensitizers clearly increases their photostability and, therefore, their photocatalytic efficiency, although they can operate through different mechanisms than those established in homogeneous conditions [10]. The wide chemical variety of organic photosensitizers has allowed them to be supported on different types of substrates such as ceramic materials, glass wool, ion exchange resins, cationic polystyrene, cellulose, and natural or synthetic fabric fibers [19–24]. Moreover, in recent years, fabric fibers have become an interesting option due to their great advantages, such as large surface area, low cost, mechanical flexibility, and easy recovery of the medium after use [25]. Literature shows examples of fabrics with photodynamic inactivation properties against different types of bacteria, viruses, and fungi by incorporating organic dyes on fabric fibers. Thus, antimicrobial fabrics such as polyester containing methylene blue, polystyrene nanofibers, and electrospun polymers dyed with tetraphenylporphyrin and also Rose Bengal (RB), used for dyeing cotton fibers, wool, and acrylic blended fibers have been reported [13,25–28]. The choice of organic photosensitizer is a critical factor for the efficiency of bacterial inactivation. Its photophysical and photochemical properties are important to design the most efficient photodynamic fabric, but its chemical structure also plays an important role in bacterial inactivation. It can generate highly reactive oxygen species (ROS) upon excitation by visible light but may, however, be ineffective for bacterial inactivation due to the electrostatic repulsion effect induced by the anionic character of photosensitizer and the cell membrane, which is negatively charged in Gram-negative bacteria but also in Gram-positive bacteria [29,30]. In this sense, RB is a very good candidate because it exhibits high singlet oxygen ($^1O_2$) quantum yield ($\Phi_\Delta = 0.76$) [31–33], and different fabrics dyed with RB have been shown to be effective in inactivating bacteria, especially Gram-positive bacteria [13,34–38]. However, no in-depth studies have been conducted that consider its chemical structure as an important factor that would advance knowledge to improve the efficiency of future photodynamic fabrics. For instance, it is known that high RB concentrations in aqueous solutions produce aggregation due to hydrophobic interactions among xanthene rings. This effect causes a self-quenching phenomenon that induces a decrease in ROS production [35] and, therefore, a reduction of the bactericidal action. In this context, the heterogenization of RB has been described as reducing aggregation-caused self-quenching [39]. Moreover, the lack of Gram-negative bacterial photoinactivation by RB heterogeneous materials has been attributed to its anionic character [40,41], but the influence of its anionic character on Gram-positive bacteria in water disinfection has never been evaluated, although the surface of their membrane also has negative charges due to the presence of compounds such as teichoic acids [29,30]. For these reasons, the aim of the present work was to determine the influence of the percentage of RB supported on polyamide fabrics (Fig. 1) in Gram-positive bacteria inactivation, considering factors such as singlet oxygen generation and the global negative charge of the material.

2. Materials and methods

2.1. Chemicals

Acetic acid (99%), dimethyl sulfoxide (DMSO, 99.8%), formic acid (98%), sodium hydroxide (97%), sodium sulfate phosphate buffer saline (PBS) and Rose Bengal disodium salt (95%) were purchased from Sigma-Aldrich. Agar-Agar from Difco™, Brain Heart Infusion (BHI), Nutrient Broth (NB), and Plate Count Agar (PCA) were purchased from Scharlab. All the solutions were prepared using water Milli-Q grade obtained from a Milli-Q® IX 7003/05/10/15.

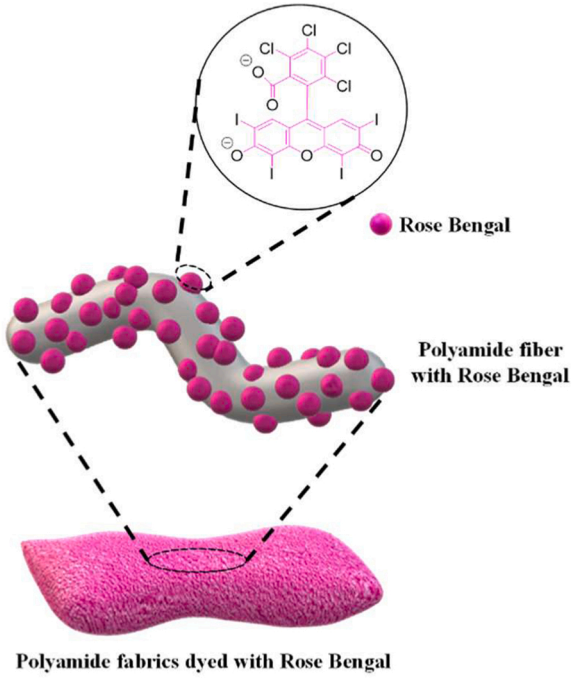

Fig. 1. Schematic illustration of polyamide fabric dyed with Rose Bengal (RB-PAF).

2.2. Dying procedure of polyamide fabrics with RB (RB-PAF)

Polyamide samples (Nylon 6.6, 5 g) were dyed with Rose Bengal (RB) according to three different intensities 0.5%, 1%, and 3% o.w.f. (on-weigth-of-fiber). The dying liquor consisted of a RB solution (1:20 w/v fabric-bath ratio) treated with 10 g/L of sodium sulfate and 5 mL/L of acetic acid to achieve a pH of 3.8. The dying device was an opened Tin Control. The liquor was heated till 100 °C, reached by a thermal gradient of 3 °C min^{-1}. The dyeing temperature (100 °C) was kept for 60 min with mechanical stirring; then, the bath was cooled to 40 °C by a thermal gradient of − 6 °C min^{-1}. Afterward, different washing cycles (4 ×100 mL) with cold Milli-Q water were made to remove excess dye and other impurities; finally, the dyed fibers were dried at room temperature.

To confirm the bath exhaustion, the amount of RB left was determined on the basis of the absorbance-concentration relationship at an absorbance of 550 nm, corresponding to the maximum absorption of RB.

2.3. Characterization of RB-PAF

2.3.1. Quantification of Dye Loading

The amount of RB adsorbed on the polyamide fabrics was determined using two different methods: UV–vis spectroscopy and inductively coupled plasma mass spectrometry (ICP-MS).

2.3.1.1. UV–vis spectroscopy. 1) Initially, the amount of RB in the fibers was calculated by subtracting the residual dye in the post-dyeing solution determined spectroscopically from the initial dye quantity.

2) To more accurately determine the amount of RB adsorbed to the polyamide fabrics, a two-step process was undertaken: i) breakage of the

fabrics, followed by ii) extraction of the dye from the broken fibers.

i) breakage of the fabrics: specific amounts of RB-PAF (0.233 g, 0.1960 g, and 0.0800 g, of 0.5%, 1%, and 3% o.w.f., respectively) were treated with 80% formic acid (2 mL) at room temperature for two minutes; then, the pH of the mixture was adjusted to 7 with NaOH (2 M). The disaggregated fabrics containing the dye were filtered and washed with Milli-Q water (5 ×100 mL).

ii) extraction of the dye from the broken fibers: the disaggregated fabrics from the previous treatment were sonicated with DMSO (20 mL) for 3 h at 80 °C. The extraction was repeated three times to ensure complete dye extraction.

The concentration of RB in the combined extracts was calculated using a calibration curve absorbance-concentration of RB in DMSO (Varian-Cary 50 spectrophotometer). Finally, the amount of RB adsorbed on the polyamide fabrics was quantified based on the absorbance of RB in the combined extracts, the total volume of the extracts, and the weight of the polyamide fabrics.

2.3.1.2. Inductively coupled plasma mass spectrometry (ICP-MS). The amount of RB adsorbed on the polyamide fabrics was determined by using an ICPMS7900 Agilent Technologies upon digestion of the fabrics and determination of the concentration of iodine (I).

2.3.2. Photometry and color measurement

In order to objectively compare color difference measurements, the chromatic coordinates [light-dark (L^*), red-green (a^*), and yellow-blue (b^*) values] of the CIELAB color space of the dyed samples were obtained using a Konica Minolta CM-3600d reflection spectrophotometer. UV (ultraviolet) energy was included. The measurements were made with the standard observer CIE-Lab 10° and the standard illuminant D65.

The chromatic coordinates are described as follows: $L = 100$ is the perfect white, and $L = 0$ belongs to black. Regarding the color, $a^* < 0$ fits with green colors, whereas $a^* > 0$ belongs to reddish shades. On the other hand, $b^* < 0$ indicates blueish colors, and $b^* > 0$ moves towards yellowish ones (Table 1). Plots from color coordinates of dyed fabrics are represented with the online software CPM 3D Plotter.

2.3.3. Diffuse reflectance

UV–vis reflectance spectra were obtained by using a Konica Minolta CM-3600d reflection spectrophotometer.

The values of color strength (K/S) of the dyed fabrics were instrumentally determined with Kubelka-Munk Eq. 1 as follows:

$$K \Big/ S = \frac{(1-R)^2}{2R} \tag{1}$$

Where R is the reflectance of the dyed fabric at the maximum absorption wavelength (λ_{max}), S is the scattering coefficient, and K is the absorption coefficient of the dyed fabrics.

2.3.4. Field Emission Scanning Electron Microscopy (FESEM)

High-resolution images of the polyamide fibers were obtained by a Field Emission Scanning Electron Microscope (FESEM, model ULTRA 55, ZEISS). Samples were prepared by covering them with a layer of gold and palladium by Sputter Coater and analyzed at an acceleration voltage of 1.5 kV and appropriate magnification.

Table 1
Visual color differences for respective differences in CIE-Lab color-difference attributes [42].

CIELAB Notation	Relevant perceptual differences	Visual perception for Positive value (+) Negative value (–)	
ΔL^*	Lightness/darkness	Lighter	Darker
Δa^*	Redness/greenness	Redder	Greener
Δb^*	Yellowness/blueness	Yellower	Bluer
ΔC^*	Chroma	Brighter	Duller

2.4. Photophysical and photodynamic studies

2.4.1. Fluorescence Spectroscopy

The steady-state and time-resolved fluorescence spectra of polyamide fabrics were carried out with an EDINBURGH INSTRUMENTS FLS 1000 equipped with a Xenon flash lamp. The fabric samples (4.5 ×1 cm) were analyzed using quartz cells for solid samples (path length 0.2, 20-C/Q/0.2 model, Starna scientific). RB fluorescence emissions were recorded using excitation wavelengths (λ_{exc}) of 366 and 500 nm. All measurements were made at room temperature, under an air atmosphere.

2.4.2. Laser flash photolysis experiments (LFP)

LFP experiments were performed using an OPO System Ekspla (EKS-NT342C-10) coupled with a UV extension (EKS-NT342C-SH-SFG) as the excitation source and an Edinburgh Instruments detection System (LP980) coupled with an ICCD camera (Andor iStar CCD 320 T).

LFP measurements of the RB-dyed fabrics (4.5 ×1 cm) were carried out with an $\lambda_{exc} = 532$ nm and a power of 10 mJ. The samples were analyzed using quartz cells for solid samples (path length 0.2, 20-C/Q/0.2 model, Starna scientific).

RB phosphorescence emissions were recorded using the ICCD camera (Andor iStar CCD 320 T) at $\lambda_{exc} = 532$ nm.

All measurements were made at room temperature, under air atmosphere.

2.4.3. Singlet oxygen generation

2.4.3.1. $^1O_2$ phosphorescence detection. The singlet-oxygen phosphorescence decay traces after the laser pulse was registered at 1270 nm employing a Peltier-cooled (@62.8 8 C) Hamamatsu NIR detector operating at 650 V, coupled to a computer-controlled grating monochromator. A pulsed Nd:YAG L52137 V LOTIS TII was used at the excitation wavelength of 355 nm. The single pulses were of ca. 10 ns duration, and the energy was lower than 5 mJ per pulse. The system consisted of the pulsed laser, a 77250 Oriel monochromator coupled to the Hamamatsu NIR detector, and the oscilloscope connected to the computer. The output signal was transferred from the oscilloscope to a personal computer. All measurements were made at room temperature, under an air atmosphere.

2.4.3.2. $^1O_2$ chemical detection. Photooxygenation of 9,10-dimethyl anthracene (DMA) was carried out in the presence of RB-PAF at 0.5% (30. 6 mg), 1% (30.7 mg) and 3% (30.1 mg) (o.w.f.) in MeCN (V= 3 mL) under stirring at 293 K in quartz cells for liquid (path length 10, 23/Q/10 model, Starna scientific). Then, the samples are irradiated in a homemade photoreactor built with a spiral set-up of 2.5 m strip green LEDs (λ_{em} centered at 520 nm), Samsung SMD2835-IP20 of 12.5 W. The average incident radiation was determined as 2.7 mW/cm^2 with a Gigahertz-Optik-P2110 radiometer with a 400–1000 nm detector (RW-3705–5). The initial concentration of DMA was 80 μM, and its absorbance was monitored by UV spectroscopy versus time, up to 60 min.

DMA photooxidation tests were also performed for the evaluation of the fabric-dyed reuse. Experiments were performed by triplicate using RB-PAF at 1% o.w.f. Thus, each piece of fabric dyed (29.3 mg, 28.7 mg, and 28.3 mg) was placed in a quartz cell (path length 10, 23/Q/10 model, Starna scientific) containing 3 mL of an 80 μM solution of DMA in MeCN. The mixtures were irradiated for 60 min at 293 K under stirring in the same homemade photoreactor (green LEDs centered at 520 nm, 2.7 mW/cm^2). After each cycle, the fabric was lightly washed with MeCN and dried, then placed again in a new 80 μM DMA solution for the next irradiation cycle. The initial and final absorbance of DMA in

each cycle was monitored by UV spectroscopy.

2.5. Antibacterial test

The bacteria, *Enterococcus faecalis* CECT184, was acquired as a liofile from the "Coleccion Española de Cultivos Tipo" (CECT) and used as a demonstrative Gram-positive strain. The reactivation of the bacterium was carried out using Brain Heart Infusion (BHI) culture media, according to the CECT instructions, and subsequently, it was grown in PCA solid medium.

For each experiment, 3–4 bacterial colonies from a PCA culture were inoculated in tubes containing 5 mL of NB and incubated at 36 ± 1 ºC in darkness. After 6–8 h, 0.5 mL of this actively growing culture was inoculated into 50 mL of NB and maintained, during 14–16 h, in the same conditions described above. Afterward, cultures were pelleted by centrifugation at 4000 rpm for 10 min at 4 °C in an Eppendorf centrifuge (5415 R; Sigma-Aldrich, Madrid, Spain). The recovered biomass was washed twice in sterile PBS and finally suspended, in the appropriate volume of PBS, to obtain a bacterial suspension containing 1×10^6 colony forming units per mL (cfu/mL), which was estimated using a Neubauer chamber. In all cases, this estimated concentration was further confirmed by a colony count in PCA.

2.5.1. Photodynamic bacterial inactivation studies

The photodynamic bacterial inactivation studies were performed against *E. faecalis* using the three polyamide fabrics dyed with RB at 0.5%, 1%, and 3% (o.w.f.).

Each sample of polyamide fabric (2.6 cm diameter, 0.0468 g) was supported in an aluminum ring in such a way the fabric was able to remain fixed and smooth during the complete experiment. The ring was immersed in a vertical position into a Pyrex vial (2.9 cm diameter, 6.5 cm height) which contained 10 mL of the bacterial suspension (1×10^6 cfu/mL in PBS). The vial was placed in the bottom of an LZC-4 photoreactor (Luzchem Research Inc., Ottawa, Canada), and the suspension was maintained in constant stirring in order to avoid bacterial precipitation (Fig. S7). Irradiations were carried out using, in side positions, 2, 4, and 8 green LZC-LED 8 Watt lamps ($\lambda_{max} = 520$ nm), which supposed irradiances, just in the point where the vial was placed, of 1.66, 3.34, and 6.75 mW/cm^2, respectively, according to the number of lamps used. Bacterial suspension aliquots (0.5 mL), which were withdrawn every 0, 5, 10, 15, and 20 min from the beginning of the irradiation, were 10-fold serially diluted using PBS. The appropriate dilutions (100 μL) were then spread plated on PCA plates and incubated at 36 ± 1 °C overnight to estimate the number of viable bacteria. Each experiment included its corresponding control performed in dark conditions. And for all the treatments, four independent repetitions were carried out. Antibacterial photodynamic activity of the fabrics is shown as survival reduction, in log (cfu/mL), throughout the experiment.

Furthermore, in those cases in which fully complete bacterial inactivation was obtained, the irradiated fabrics were directly placed on PCA plates and incubated, as described above, to confirm whether all the bacteria that could have been attached to the fabric throughout the experiment were really inactivated.

2.5.2. Effect of RB concentration in the fabrics on their capability to adsorb bacteria

To determine whether the RB concentration in the fabric could affect its capability to adsorb bacteria, two fabrics (1 cm^2 surface) of the RB concentrations, 1% and 3% (o.w.f.), were evaluated by using an *E. faecalis* concentration of 1×10^3 cfu/mL in 4 mL of PBS. The experiments were carried out in glass vials (2.0 cm diameter x 2.5 cm height), in constant stirring (200 rpm), at room temperature (22 ± 1 °C). The number of bacteria remaining in the suspension after different experimental periods was determined. Thus, aliquots (1 mL) were withdrawn after 0, 1, and 2 h from the beginning of the experiment. Bacteria in the suspensions were established through viable count by placing, directly from the aliquot or from the appropriate dilution, 100 or 50 μL on PCA plates and incubated overnight at 36 ± 1 °C. The number of bacteria adsorbed on the fabric was calculated by subtracting the cfu/mL in the bacterial suspension after the evaluated period from the cfu/mL at the beginning of the experiment. All experiments were independently repeated 4 times.

2.5.3. Evaluation of the antibacterial durability of the photodynamic fabrics

In order to appraise the RB-PAF 1% o.w.f. durability for its repeated and long-term usage, *E. faecalis* inactivation studies were performed after 1, 4, 7, and 10 disinfection cycles. Hence, all the disinfection cycles were carried out as described in the photodynamic bacterial inactivation studies section, but only in the mentioned 1st, 4th, 7th, and 10th cycles the *E. faecalis* inactivation was quantified. All cycles were done by using 8 lamps and an irradiation time of 15 min. After each cycle, the fabric was rinsed with sterile distilled water (2 ×20 mL), directly introduced into newly-made bacterial suspension (1×10^6 cfu/mL; 10 mL), and subjected to the next irradiation cycle. The experiment was performed in quadruplicate.

2.6. Data statistical analysis

Antibacterial photodynamic activity of RB-PAF 1% o.w.f. obtained after exposure to different green-light irradiances throughout different time periods was analyzed by conducting a Welchś ANOVA [43]. Games-Howell post hoc-analysis subsequently established the statistically significant differences ($P < 0.05$). This study was performed by using the statistical package SPSS v.16.0.1 (2008). SPSS Inc.

On the other hand, one-way ANOVA followed by the Tukeýs Honestly Significant Difference (HSD) Test [44] was used to establish differences in the experiment of antibacterial durability of the photodynamic fabric as well as the Studentś *t*-test [45] was used to compare results in the experiment of bacteria adsorption on fabrics. In this case, analysis was performed by using the statistical package Statgraphics Centurion v. 18.1.13. (2018). Statgraphics Technologies Inc.

3. Results and discussion

3.1. Characterization of polyamide fabrics dyed with Rose Bengal

The main objective of this work was to evaluate the efficiency of polyamide fabrics dyed with different concentrations of Rose Bengal (RB-PAF) for the inactivation of Gram-positive bacteria. The percentages of RB incorporated into the polyamide fabric were selected in the range of the values of most dyed fabrics described in the literature [26,38,46]. For this purpose, three different initial concentrations of RB were used. Table 2 shows the loading of the RB on the fabrics determined by three different methods. Dyeing corresponds to the loadings spectroscopically determined by subtracting the residual dye in the post-dyeing solution from the initial dye quantity. Although this process of dye quantification using spectroscopic techniques by analyzing the wash water is widely used in the textile industry, other chemical methods to extract and quantify the dye from fabrics were also carried out in a complementary manner. Fig. S1 shows the evolution of RB-PAF to chemically extract RB. Upon the first treatment with formic acid, the fibers are broken due to hydrolysis and protonation of the RB, resulting in a colorless

Table 2
Concentration of RB on the polyamide fabric.

Theoretical Dyed polyamide fabric (% o.w.f.)	*Dyeing (% o.w.f.)*	*Extraction (% o.w.f.)*	*ICP-MS (% o.w.f.)*
0.5	0.500	0.59	0.58
1.	0.985	1.29	0.99
3	2.638	3.33	3.00

disaggregated fiber (image not shown). Nevertheless, the color was recovered upon neutralization (Fig. S1B). Afterward, three consecutive extractions with DMSO solvent were needed to produce a complete extraction of the dye, interrupting the physical interaction between the dye (RB) and the polyamide fibers (see images S1C, S1D, and S1E after each consecutive extraction) [47]. The absorbance of the combined extracts allowed for determining the concentration using a calibration curve of RB in DMSO (Fig. S2A). The RB loadings determined for each RB-PAF are shown in Table 2. Finally, the amount of RB on fabrics was also determined by inductively coupled plasma mass spectrometry (ICP-MS). The differences in RB loading obtained by the three methods are slightly different; while the quantification by absorbance difference between the dying bath and the washes seems to underestimate the concentration of RB, the chemical extraction overestimates the theoretical values. Nevertheless, the values obtained from the ICP-MS seem to accurately give reasonable results as it is an analytical technique that has a low detection limit and can detect trace elements.

The three RB-PAFs were compared against the white fabric. Results in Table 3 show colorimetric coordinates for every sample, including the white one. It is observed how the L^* moves towards lower values which indicates darker samples. The higher the amount of dyeing, the lower values for L^*, which is consistent with the higher concentration of the darker sample. It is seen how dyed samples show $Da^* > 0$, which is directly related to reddish samples. However, $Db^* < 0$, especially for low concentrations of dye, implies the sample is yellowish than samples with a higher concentration of dye. As should be expected $DEab^*$ offers a direct relationship with dye concentration; the higher concertation of dye, the higher the color difference.

Results in Fig. S3 show the final coordinates of fabrics once they have been dyed at different concentrations (3%, 1%, 0.5%). Table 3 shows the objective measurement of differences between plots. In this case, the reference or control is the white fabric (not dyed). The fabric with a higher amount of dye should show a higher color difference with white. Surprisingly, as can be seen in Table 3, polyamide dyed at 3% (red plot in Fig. S3) shows lower DL^* or $DEab^*$ than polyamide dyed at 1% (o.w.f.) (orange plot in Fig. S3 when compared with control fabric (white).

The color depth of the three RB-PAFs was obtained by measuring the reflectance of light. Fig. 2 shows that the results for the three polyamide fabrics are in parallel with the nominal RB loading. In all cases, the maximum absorption of RB on RB-PAF (λ_{max}= 560 nm) exhibited a bathochromic shift of 14 nm compared to the aqueous solution with a λ_{max}= 546 nm (Fig. S4). However, the ratio between the maximum at 525 and the maximum at 560 nm clearly increases from RB-PAF at 0.5% (o.w.f.) (blue) to 1% (o.w.f.) (red) and to 3% (o.w.f.) (black). This behavior may be interpreted in terms of dye aggregation [48].

The FESEM technique was used to investigate the surface morphology of RB-PAF. Fig. S5 shows a typical homogeneous fiber of the synthetic fabric with 1% (o.w.f.) before (Fig. S5A) and after the dyeing process (Fig. S5B). As it can be concluded from the comparison of the two figures, the association of RB to the fiber did not affect its morphology.

3.2. Photophysical properties of polyamide fabrics dyed with Rose Bengal

Steady-state and time-resolved emission measurements, as well as laser flash photolysis experiments, including the detection of RB triplet excited state (^{3}RB*) and singlet oxygen ($^1O_2$) generation, were performed to determine the effect of the different percentages of RB on the polyamide fabric in the photophysical properties of the dye. Thus, steady-state fluorescence emission spectra of RB-PAF (Fig. 3A) show a bathochromic shift compared to the homogeneous RB (λ_{max} = 567 nm) in aqueous media [49,50]. This redshift of the fluorescence maximum is dependent on the percentage of RB loading in the polyamide fabric ($\lambda_{0.5\%}$ and $\lambda_{1\%}$ ca. 610 nm and $\lambda_{3\%}$ = 628 nm). The bathochromic effect may be due to the dependence of the photophysical properties of the photosensitizers to the fixation on the fabric and the distance between the chromophore units, which decreases with increasing loading percentage, thus hindering conformational changes between their transition states. It has been observed in various xanthene dyes on different materials (cotton fabric, wool/acrylic fabric, cellulose, etc.) [48,51,52]. The observed emission maximum is red-shifted, and the amplitude of the red tail increases with respect to the main band, as expected when increasing the percentage of RB leads to reabsorption of luminescence [48]. The observed steady-state emission results pointed to the aggregation of RB in the fabrics. Nevertheless, the time-resolved fluorescence experiments (Fig. 3B) performed in an air atmosphere (λ_{exc} = 500 nm) showed a decrease in the fluorescence lifetimes (τ_f) when the percentage of RB in the different RB-PAF increased from 0.5% to 3% (o.w.f.), (1.5, 1.4 and 1.0 ns respectively). These time-resolved data acted as an unambiguous piece of evidence that a charge transfer interaction between RB singlet excited state and close ground state RB moieties is happening, which is the most likely deactivation pathway of the first singlet excited state of photosensitizers supported in heterogeneous materials [53]. Accordingly, it is expected that RB triplet excited state quantum yield was considerably lower for RB-PAF at 3% than the one at 0.5% (o.w.f.).

Laser flash photolysis (LFP) studies were performed on the fabrics to observe the formation of RB triplet excited state (^{3}RB*) because its detection anticipates singlet oxygen generation. Thus, the transient absorption of polyamide fabrics dyed at RB 0.5%, 1%, and 3% (o.w.f.) was recorded at different times after the laser pulse using the spectral detection range of 300–800 nm at the excitation wavelength of 532 nm

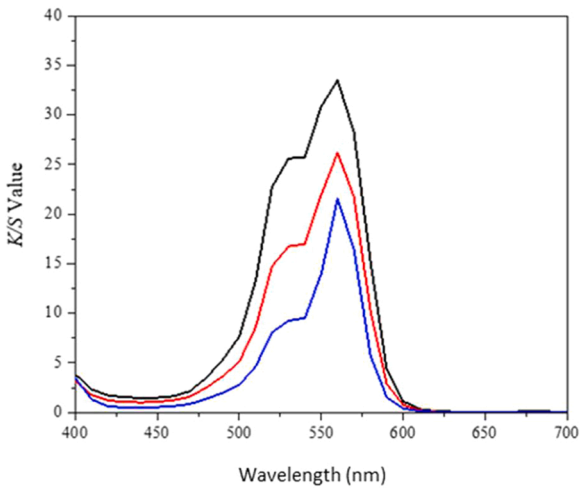

Fig. 2. *K/S* vs wavelength curves of RB-PAF at 0.5% (o.w.f.) (blue), 1% (o.w.f.) (red), and 3% (o.w.f.) (black).

Table 3
CIELAB Values of RB on the polyamide fabric (RB-PAF).

	L^*	a^*	b^*	DL^*	Da^*	Db^*	$DEab^*$
Control*	93.1609	3.0462	-13.0825				
0.5%	49.1587	62.478	-24.9276	-44.0022	59.4318	-11.8451	74.8908
1%	44.1889	64.0353	-17.4385	-48.972	60.9891	-4.356	78.3384
3%	40.7891	64.0125	-14.9584	-52.3718	60.9663	-1.8759	80.3941

* Undyed polyamide fabrics.

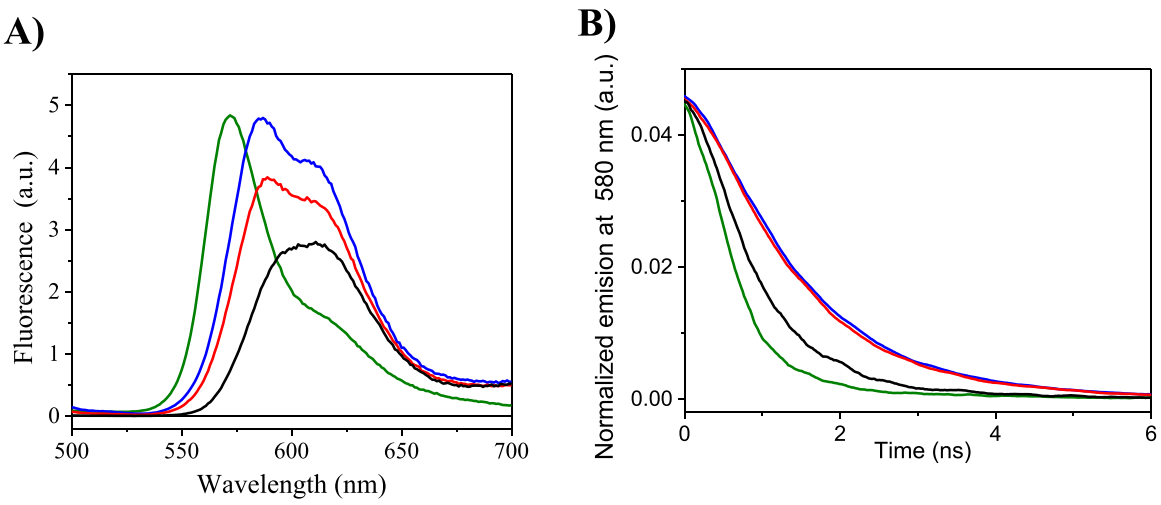

Fig. 3. Steady-state (A) and time-resolved (B) fluorescence emission spectra of RB-PAF at 0.5% (o.w.f.) (blue), 1% (ow.f.) (red), and 3% (o.w.f.) (black). Homogeneous RB (green) as control at Abs = 2 at λ_{exc}= 500 nm in H_2O.

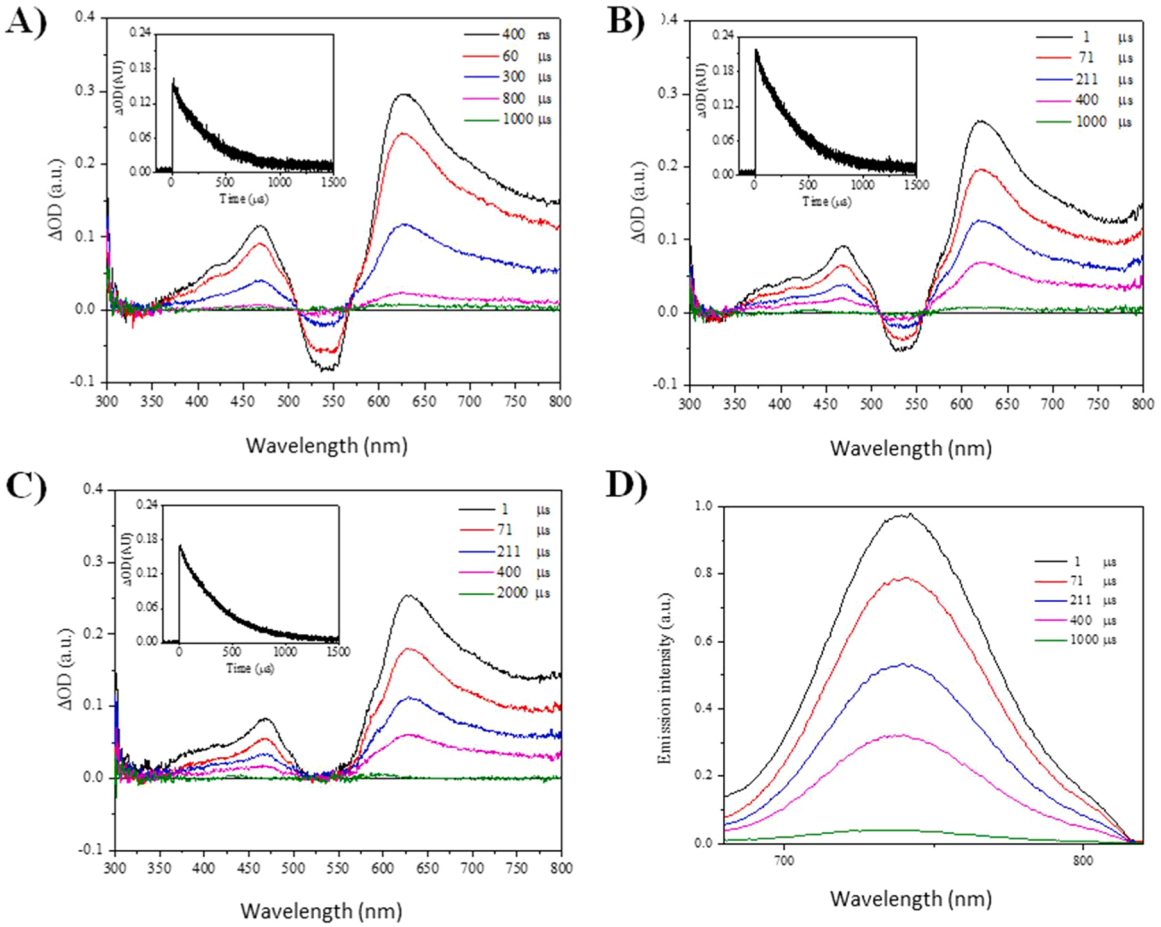

Fig. 4. Transient absorption spectra of polyamide fabrics dyed at (A) 0.5%, (B) 1%, (C) 3% (o.w.f.) of RB, and (D) phosphorescence emission at 1% (o.w.f.) of RB obtained at different times after the laser pulse at λ_{exc}= 532 nm in solid under air. The insets show the corresponding ^{3}RB* decay traces recorded at 600 nm.

(Fig. 4). The three RB-PAF showed intense absorption maxima at ca. 475 and 625 nm and bleaching centered at ca. 540 nm. The bleaching intensity decreases by increasing the RB load on the fabric, but this fact can be attributed to the higher light absorption by the more loaded fabrics. The observed absorption spectrum in the three fabrics can be attributed to the ^{3}RB* since it is similar to that observed for homogeneous RB regardless of the nature of the employed solvent [54,55]. Interestingly, the ^{3}RB* detected in RB-PAF show similar lifetimes (275, 282, and 275 μs for RB 0.5%, 1%, and 3% (o.w.f.), respectively, under aerated media), and they also resulted in being almost the same under nitrogen than in air atmosphere. The fact that the ^{3}RB* is not quenched by oxygen in the three fabrics has not been previously described for dyes heterogeneously supported because this type of material has never been studied by the laser flash photolysis technique. In this context, further

support for the ^{3}RB* behavior was observed when phosphorescence measurements were performed at the same time that the ^{3}RB* absorption spectra. Thereby, as is shown in Fig. 4B and 4D, the emission spectrum of the RB phosphorescence observed at λ_{max} ca. 737 nm [56] decays at the same time that the absorption spectrum of ^{3}RB*.

Singlet oxygen generation from the fabrics was monitored by the typical singlet-oxygen phosphorescence at $\lambda = 1270$ nm generated by pulsed-laser irradiation in aerated media. Thus, all decays showed lifetimes of ca. 270 μs, which agree with those determined for ^{3}RB* lifetimes (results not shown).

3.3. Photodynamic studies

Although spectroscopic techniques have evidenced the involvement of ^{3}RB* in the generation of $^1O_2$, it was impossible to quantify the efficiency of the processes in the three RB-PAFs. Hence, a chemical method to indirectly quantify the singlet oxygen generation of photosensitizer was performed. This chemical method is based on the photooxygenation of 9,10-dimethyl anthracene (DMA) to its corresponding endoperoxide (Scheme S1). This experiment revealed that the singlet oxygen generation is dependent on the RB percentage on fabrics, in the order: of 1% > 3% > 0.5% (o.w.f.) (see results in Fig. 5). Therefore, the lowest % of RB produces a very low DMA photooxygenation, while the highest % of RB does not show better results than that obtained using RB 1%. The result obtained at RB 3% can be attributed to RB π-π stacking and aggregation [57], which agrees with the photophysical results previously commented. The close proximity between ^{1}RB* and RB ground state gives rise to a self-quenching effect of the excited state that decreases the efficiency of intersystem crossing and, consequently, the $^1O_2$ generation. Thus, the percentage of supported dye in a heterogenization process remains a critical factor in optimizing the efficiency of the photodynamic activity.

In addition, recycling experiments performed with RB-PAF 1% o.w.f. in the photooxidation reaction of DMA to its corresponding endoperoxide for 60 min under green LED irradiation (Fig S6), revealed that the fabric kept good efficiency up to 7 consecutive catalytic cycles (60–40%). This smaller reduction in the intensity of the DMA signal during the successive cycles is directly related to the loss of the pink color of the fabric that has been observed. Therefore, this fabric has the potential of generating reactive oxygen species continuously during long irradiation times.

3.4. Inactivation of bacteria by RB-PAF

After determining the photophysical properties of RB-PAF and performing DMA photodynamic studies, it is clear that these RB-supported materials are able to generate singlet oxygen, and in consequence, they would be able to produce bacterial photoinactivation. Hence, experiments against the Gram-positive bacteria, *E. faecalis*, were conducted in order to appraise the effect of the percentage of RB in the fabric using

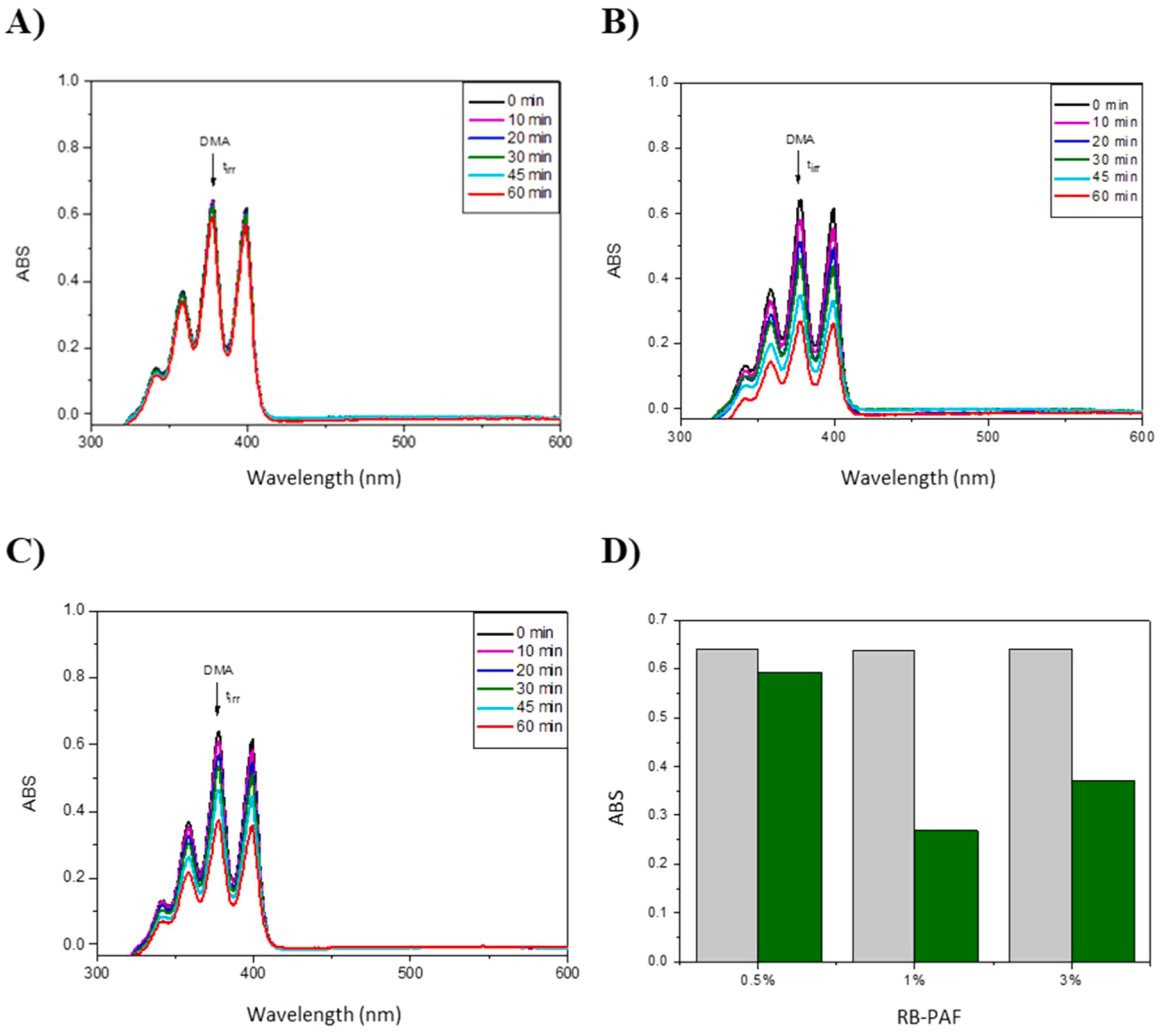

Fig. 5. Absorbance of the DMA (80 μM, in MeCN) in the presence of RB-PAF 0.5% (A), 1% (B), and 3% o.w.f. (C), V = 3 mL, upon irradiation time, with green LED light under air. Comparison of the decrease in DMA absorbance (recorded at 376 nm) at 0 (grey) and after 60 min of irradiation (green) with all fabrics (D).

different green-light irradiation doses.

Kinetic results obtained with bacterial suspensions containing RB-PAF 1% o.w.f. at different irradiation doses are shown in Fig. 6. The antibacterial activity of the fabric proportionally increased as both irradiance and time increased. For each recorded time, Welch's one-way ANOVA was conducted to determine if the change of activity due to the irradiation factor was statistically significant. This statistical test was chosen here because, although in all cases, data were normally distributed, the assumption of homogeneity of variances was violated as assessed by Levene's Test of Homogeneity of Variances (Table S1). The statistical analysis revealed that, after 5 min of treatment, the three different irradiation doses were able to activate the fabric, provoking bacterial survival reductions statistically different, according to Games-Howell post-hoc analysis, to that of the non-irradiated control (Table S1 and S2). Moreover, the fabric exposed to 8 lamps (Fig. S7) for 5 min was able to reduce the survival by almost 3 $\log_{10}$ units and was statistically more active than the other two irradiated fabrics with 2 and 4 lamps, which performed similar results ($P = 0.056$). From 10 min onwards, all the treatments showed statistically significant differences between each other (Table S1 and S2). Thereby, RB-PAF 1% o.w.f. showed a potent antibacterial efficiency. In fact, no bacteria colonies were recorded in the viable counts (100% inactivation activity) after exposure to an irradiance of 6.75 mW/cm^2 at just 15 min (Fig. 6, dark pink trace). However, the fabric loaded with the lowest concentration (RB-PAF 0.5% o.w.f.) exhibited non-bacterial inactivation under none of the tested irradiation conditions, including the highest irradiation dose (6.75 mW/m^2 during an extended period of 60 min, Fig. S8A). Interestingly, RB-PAF at 3% o.w.f. only showed 1 $\log_{10}$ unit reduction (90% activity) at the highest irradiation dose (Fig. S8B). All samples were also evaluated in darkness, and bactericidal activity was not detected in any cases.

Although no viable bacteria were recovered from the bacterial suspension containing RB-PAF 1% after 15 min using the light intensity of 6.75 mW/m^2, to confirm the complete bacterial inactivation, fabrics coming from this experiment were incubated in PCA in order to evaluate whether all bacteria remaining adhered to the fabric surface had been really killed by the photodynamic action. Results showed that the fabric did not contain any viable bacteria because no growth was recorded after 24–48 h of incubation (Fig. S9). This result allows us to unambiguously conclude that the RB-PAF 1% (o.w.f.) is able to reduce bacterial concentration by more than 6 $\log_{10}$ units which, in our experimental conditions, supposes 100% bacterial inactivation.

The above results have proven that the concentration of RB in the fabric is a crucial factor for determining its photodynamic bactericidal activity and that a narrow margin of active concentrations exists. In this way, while RB-PAF 1% (o.w.f.) has a remarkable antibacterial activity, a reduction of only half the concentration (0.5% o.w.f.) produced a complete loss of activity. On the other hand, an increase of approximately 3 times the active concentration markedly reduced the antimicrobial activity.

The bactericidal activity results are in good correlation with those arising from determinations of $^1O_2$, where the amount of singlet oxygen generated for RB-PAF follows the order: 1% ≥ 3% > 0.5% o.w.f. Hence, the antibacterial activity of RB-PAF could be ascribed to the capability to sensitize oxygen [39]. However, although the lack of activity showed by RB-PAF 0.5% can be clearly attributed to the fact that the amount of dye in this fabric is not able to generate enough $^1O_2$ to kill the bacteria, the very low activity of RB-PAF 3% can not only be attributed to singlet oxygen generation because its value is very close to that determined for RB-PAF 1%.

3.5. Capability of the functionalized fabrics to adsorb bacteria

As commented above, the loss of bactericidal activity in RB-PAF 3% cannot be clearly understood only by the small singlet oxygen generation decrease observed for RB-PAF 3% by comparing to that of RB-PAF 1%. Thus, another event ought to be taking place, and because of this, it was postulated that the increasing amounts of RB on the fabric surface would increase its negative net charge due to the anionic character of the dye. This fact could prevent bacteria, which possess a negatively charged surface, from approaching the fabric surface. To prove this hypothesis, the number of bacteria adsorbed on RB-PAF 1% and 3% were quantified, in dark conditions, by using a bacterial suspension containing 1 × 10^3 cfu/mL. This low bacterial concentration was used in order to obtain more accurate measurements than those obtained when concentrations are high, and saturation effects on the fabric surface may be happening.

Fig. 7 shows the percentage of bacteria adsorbed on RB-PAF 1% and 3% when exposed to the bacterial suspension during 1 and 2 h in darkness. As expected, RB-PAF 1% showed higher levels of bacteria adsorption than those exhibited by RB-PAF 3% at both exposure times. Thus, after 1 h of treatment, RB-PAF 1% was able to adsorb 86.6% of bacteria contained in the suspension, while RB-PAF 3% only reached an adsorption mean value of 58.8%, which was statistically smaller than the former ($t = 16.13$; $P = 0.00008$). Furthermore, after 2 h of exposure, the statistical difference became bigger as the adsorption level in RB-PAF 1% increased up to 98.9%, but that of RB-PAF 3% remained unchanged ($t = 20.71$; $P = 0.00003$). The behavior of bacteria adsorption in RB-PAF 3% should be compatible with a higher electrostatic repulsion phenomenon enhanced by a higher load of the anionic dye. This event is important from the point of view of the loss of photodynamic activity as

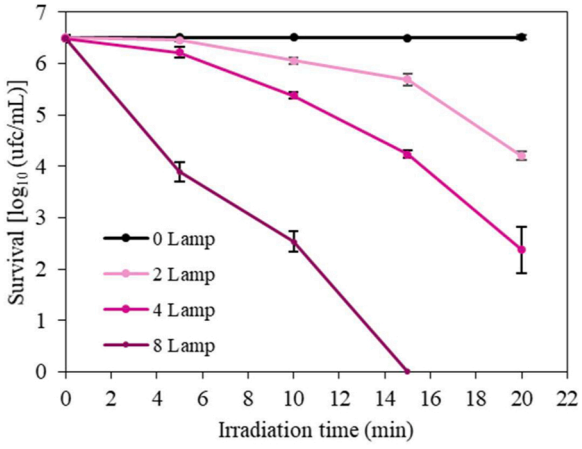

Fig. 6. Survival reduction of *Enterococcus faecalis* exposed to Rose Bengal-Polyamide Fabric 1% o.w.f., irradiated using different light intensities: 1.66 (2 lamps; pale pink trace), 3.34 (4 lamps; pink trace), and 6.75 mW/cm^2 (8 lamps; dark pink trace). Control experiment in dark conditions is shown in black.

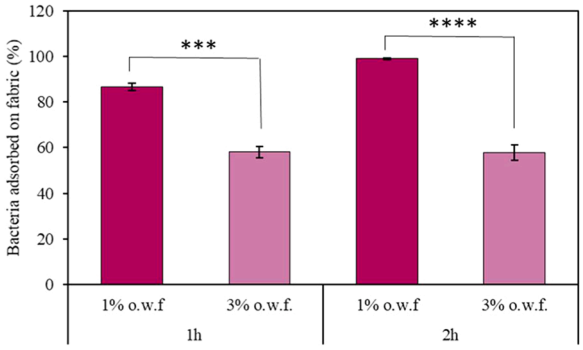

Fig. 7. Percentage of bacteria adsorbed (mean ± standard deviation; n = 3) on dyed polyamide fabric at 1% (o.w.f.) and 3% (o.w.f.) in dark conditions. Experiments were performed by using an *E. faecalis* concentration of 1 × 10^3 cfu/mL. Mean values being statistically different: * ** ($P < 0.0005$) and * ** * ($P < 0.00005$).

the lifetime of singlet oxygen in water is very short (3.45 μs at 25 °C) [58], and it is the close contact that makes it easier for the singlet oxygen to inactivate bacteria. Therefore, as electrostatic repulsion increases, photodynamic activity should notably decrease.

Other previous works have observed that increasing the percentage of Rose Bengal in other types of fibers above 3% o.w.f. did not improve the inactivation efficiency of other Gram-positive bacteria, such as *Staphylococcus aureus* [13,38], an effect that could be attributed to a strong electrostatic repulsion and, consequently, to their difficulty to adhere to the fabrics, as it was observed in this work. Therefore, considering all the results of this study, the Gram-positive bacteria are considerably adhered on the surface of RB-PAF 1% (o.w.f.) due to a low electrostatic repulsion effect, and then singlet oxygen generated upon irradiation produces its inactivation within 15 min (Scheme 1). However, recent studies have proven that the occurrence of RB-Type I photoreactions, under specific conditions, could be prominent, and they could be playing an important role in reaching a more potent antibacterial activity [59,60]. In light of this evidence, the involvement of Type I photoreactions in our experiments should not be ruled out.

3.6. Antibacterial durability of the photodynamic fabric

Practical applications of this potential photodynamic fabric for wastewater disinfection require the possibility of long-term usage. In this sense, we performed experiments to quantify the degree of photosensitized inactivation of bacteria at different disinfection cycles (Fig. 8). As previously mentioned, during the first disinfection cycle, the fabric was able to inactivate all the bacteria contained in the suspension, which means a bacteria reduction of more than 6 $\log_{10}$ units in only 15 min. After three further cycles, RB-PAF was active enough to reduce 2.64 $\log_{10}$ units, according to which the bactericidal efficacy of the fabric was still 46.8% with respect to that of the first use. Interestingly, this effectiveness remained stable over the six following disinfection cycles, reaching bacterial reductions of 2.3 and 2.8 $\log_{10}$ units after the seventh and tenth cycles, respectively. In fact, statistical analysis of the obtained results revealed that the bactericidal activity of the fabric was statistically different throughout the experiment ($F_{3,\ 12} = 56.49$; $P = 0.0000$), but the only value being significantly different to the other ones was that belonging to the first disinfection cycle (Fig. 8).

These results, which have proven almost a 50% of initial efficacy in the fabric after, at least, 10 disinfection cycles, suggest a feasible practical applicability. However, based on the own nature of this catalyst, it seems reasonable to think that modifications allocated to extend the useful life of this photodynamic fabric would be relatively easy to obtain.

Based on the important level of antibacterial activity obtained, RB-PAFs could suppose a starting point in the development of an adequate tool for wastewater disinfection. Polyamide fabric shows different advantages, such as being a low-cost and highly wear-resistant

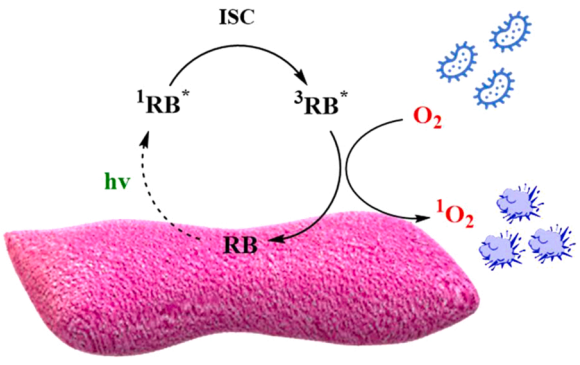

Scheme 1. The proposed mechanism of RB-PAF for the inactivation of Gram-positive bacteria is Type II (energy transfer to form singlet oxygen).

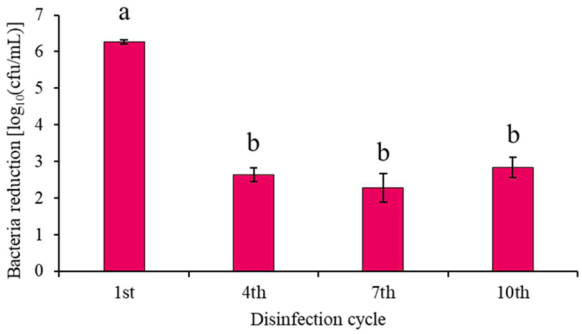

Fig. 8. Capability of Rose Bengal-Polyamide Fabric 1% o.w.f. to reduce the *Enterococcus faecalis* concentration after several disinfection cycles. Initial bacteria concentration was always around 1×10^6 cfu/mL. Results are represented as mean ± standard error (n = 4). Bars bearing different letters are statistically different ($P < 0.05$).

material. However, that option will only be feasible whether RB-PAF bactericidal activity spectrum can encompass Gram-negative bacteria as RB-PAFs were inactive against our representative Gram-negative bacteria (*Escherichia coli*) when assayed in the same conditions as those used against *E. faecalis* (data non-shown). This lack of activity against Gram-negative bacteria can be easily solved by introducing, into the fabric, cationic functionalities from polymeric or non-polymeric materials. These antimicrobial products establish synergies with the photosensitizer, drastically increasing the photodynamic activity against Gram-negative bacteria [23,34]. Following this way, works are in progress in order to feature RB-PAF as a new tool for wastewater disinfection.

4. Conclusions

Polyamide fabrics dyed with an anionic photosensitizer, such as Rose Bengal, were prepared at three different concentrations of 3%, 1%, and 0.5% (o.w.f.), and their CIELab color coordinates (positive a^* and b^* values) determined the red color of the fabrics. When the three polyamide fabrics were tested, only the fabric dyed with 1% RB (o.w.f.) achieved a high capacity for photoinactivation of Gram-positive bacteria (*E. faecalis*), reporting a photoinactivation of 6 $\log_{10}$ reduction units in cfu/mL irradiated under visible light at 6.75 mW/cm^2 in 15 min. However, the fabrics with 0.5% and 3% (o.w.f.) did not show efficacy, or only a small quantity, respectively, for bacterial inactivation. Photophysical and photodynamic studies with bacteria have determined that the amount of photosensitizer on the support plays a crucial role in bacterial inactivation. A lower amount of RB does not generate sufficient singlet oxygen, while a higher amount can be counterproductive by causing aggregation of the photosensitizer, which also leads to a decrease in singlet oxygen formation. In this latter case, moreover, an appreciable rise in the net negative charge of the fabric due to the anionic character of RB induces a higher electrostatic repulsion with bacteria which contributes to impairing the antibacterial photodynamic response of the fabric. This work opens the opportunity to design and develop more efficient photodynamic fabrics for water disinfection, where there is better control of the percentage of photosensitizer or to create synergies with other elements that reduce the electrostatic repulsion with bacteria.

CRediT authorship contribution statement

Jenny Flores: Investigation, Methodology, Writing – original draft; **Alberto Blázquez-Moraleja:** Investigation, Writing – original draft, Methodology, Validation, **Marilés Bonet-Aracil:** Conceptualization, Writing – original draft, Funding acquisition, Validation; **Pilar Moya:** Conceptualization, Writing – original draft, Funding acquisition,

Validation; **Francisco Bosca:** Conceptualization, Funding acquisition, Project administration, Supervision, Validation, Writing – review & editing, **M. Luisa Marin:** Conceptualization, Funding acquisition, Project administration, Supervision, Validation, Writing – review & editing.

Declaration of Competing Interest

The authors declare that they have no known competing financial interests or personal relationships that could have appeared to influence the work reported in this paper.

Data Availability

Data will be made available on request.

Acknowledgments

We are grateful for the CONACYT doctoral fellowship for J. F. (709358), and we also thank the Universidad Complutense de Madrid, Ministry of Universities, and Next GenerationEu recovery plan for financial support for the postdoctoral contract "Margarita Salas" for the requalification of the Spanish University System (CT31/21, 2021–2023), the Spanish Ministry of Science and Innovation (PID2019–110441RB-C33 funded by MCIN/AEI/10.13039/501100011033), and to the Valencian Agency for Innovation (INNEST/2021/75). Finally, we would also like to thank the CRUE-Universitat Politècnica de València for funding the open access fee.

Appendix A. Supporting information

Supplementary data associated with this article can be found in the online version at doi:10.1016/j.jece.2023.110639.

References

[1] Drinking-water, (n.d.). https://www.who.int/en/news-room/fact-sheets/detail/drinking-water (accessed March 9, 2023).
[2] C.A. del Valle, V. Pérez-Laguna, I.M. Resta, R. Gavara, C. Felip-León, J.F. Miravet, A. Rezusta, F. Galindo, A cost-effective combination of Rose Bengal and off-the-shelf cationic polystyrene for the photodynamic inactivation of Pseudomonas aeruginosa, Mater. Sci. Eng.: C. 117 (2020), 111302, https://doi.org/10.1016/j.msec.2020.111302.
[3] O. Planas, R. Bresolí-Obach, J. Nos, T. Gallavardin, R. Ruiz-González, M. Agut, S. Nonell, Synthesis, photophysical characterization, and photoinduced antibacterial activity of methylene blue-loaded amino- and mannose-targeted mesoporous silica nanoparticles, Molecules 20 (2015) 6284–6298, https://doi.org/10.3390/molecules20046284.
[4] S. Sharma, A. Bhattacharya, Drinking water contamination and treatment techniques, Appl. Water Sci. 7 (2017) 1043–1067, https://doi.org/10.1007/s13201-016-0455-7.
[5] Y. Zhao, Z.-X. Low, Y. Pan, Z. Zhong, G. Gao, Universal water disinfection by piezoelectret aluminium oxide-based electroporation and generation of reactive oxygen species, Nano Energy 92 (2022), 106749, https://doi.org/10.1016/j.nanoen.2021.106749.
[6] R. Dewil, D. Mantzavinos, I. Poulios, M.A. Rodrigo, New perspectives for advanced oxidation processes, J. Environ. Manag. 195 (2017) 93–99, https://doi.org/10.1016/j.jenvman.2017.04.010.
[7] J. Byrne, P. Dunlop, J. Hamilton, P. Fernández-Ibáñez, I. Polo-López, P. Sharma, A. Vennard, A Review of Heterogeneous Photocatalysis for Water and Surface Disinfection, Molecules 20 (2015) 5574–5615, https://doi.org/10.3390/molecules20045574.
[8] M.C.V.M. Starling, R.P. de Mendonça Neto, G.F.F. Pires, P.B. Vilela, C.C. Amorim, Combat of antimicrobial resistance in municipal wastewater treatment plant effluent via solar advanced oxidation processes: achievements and perspectives, Sci. Total Environ. 786 (2021), 147448, https://doi.org/10.1016/j.scitotenv.2021.147448.
[9] A. Kulišťáková, Removal of pharmaceutical micropollutants from real wastewater matrices by means of photochemical advanced oxidation processes – a review, J. Water Process Eng. 53 (2023), 103727, https://doi.org/10.1016/j.jwpe.2023.103727.
[10] A. Blázquez-Moraleja, O. Cabezuelo, R. Martinez-Haya, L.C. Schmidt, F. Bosca, M. L. Marin, Organic photoredox catalysts: tuning the operating mechanisms in the degradation of pollutants, Pure Appl. Chem. 0 (2023), https://doi.org/10.1515/pac-2022-1206.
[11] E. Koh, R. Fluhr, Singlet oxygen detection in biological systems: Uses and limitations, Plant Signal Behav. 11 (2016), e1192742, https://doi.org/10.1080/15592324.2016.1192742.
[12] O. Legrini, E. Oliveros, A.M. Braun, Photochemical processes for water treatment, Chem. Rev. 93 (1993) 671–698, https://doi.org/10.1021/cr00018a003.
[13] W. Chen, J. Chen, L. Li, X. Wang, Q. Wei, R.A. Ghiladi, Q. Wang, Wool/Acrylic blended fabrics as next-generation photodynamic antimicrobial materials, ACS Appl. Mater. Interfaces 11 (2019) 29557–29568, https://doi.org/10.1021/acsami.9b09625.
[14] I. Okamoto, H. Miyaji, S. Miyata, K. Shitomi, T. Sugaya, N. Ushijima, T. Akasaka, S. Enya, S. Saita, H. Kawasaki, Antibacterial and antibiofilm photodynamic activities of lysozyme-Au nanoclusters/Rose bengal conjugates, ACS Omega 6 (2021) 9279–9290, https://doi.org/10.1021/acsomega.1c00838.
[15] F. Vázquez-Ortega, I. Lagunes, Á. Trigos, Cosmetic dyes as potential photosensitizers of singlet oxygen generation, Dyes Pigments 176 (2020), 108248, https://doi.org/10.1016/j.dyepig.2020.108248.
[16] S. Gnanasekar, G. Kasi, X. He, K. Zhang, L. Xu, E.-T. Kang, Recent advances in engineered polymeric materials for efficient photodynamic inactivation of bacterial pathogens, Bioact. Mater. 21 (2023) 157–174, https://doi.org/10.1016/j.bioactmat.2022.08.011.
[17] M.B. Spesia, E.N. Durantini, Evolution of phthalocyanine structures as photodynamic agents for bacteria inactivation, Chem. Rec. 22 (2022), https://doi.org/10.1002/tcr.202100292.
[18] R.T. Aroso, F.A. Schaberle, L.G. Arnaut, M.M. Pereira, Photodynamic disinfection and its role in controlling infectious diseases, Photochem. Photobiol. Sci. 20 (2021) 1497–1545, https://doi.org/10.1007/s43630-021-00102-1.
[19] A. SOLEIMANIGORGANI, J. TAYLOR, Dyeing of nylon with reactive dyes. Part 2. The effect of changes in level of dye sulphonation on the dyeing of nylon with reactive dyes, Dyes Pigments 68 (2006) 109–117, https://doi.org/10.1016/j.dyepig.2005.01.014.
[20] Y. Guo, S. Rogelj, P. Zhang, Rose Bengal-decorated silica nanoparticles as photosensitizers for inactivation of gram-positive bacteria, Nanotechnology 21 (2010) 65102, https://doi.org/10.1088/0957-4484/21/6/065102.
[21] Z. Yan, W. Wei, H. Xun, S. Anguo, Rose bengal immobilized on wool as an efficiently "green" sensitizer for photooxygenation reactions, Chem. Lett. 41 (2012) 1500–1502, https://doi.org/10.1246/cl.2012.1500.
[22] V. Cardoso, T. Rittmeyer, R.J. Correa, G.C. Brêda, R.V. Almeida, G. Simões, B.M. de França, P.N. de Azevedo, J.S.Bello Forero, Photoactive cotton fabric: Synthesis, characterization and antibacterial evaluation of anthraquinone-based dyes linked to cellulose, Dyes Pigments 161 (2019) 16–23, https://doi.org/10.1016/j.dyepig.2018.09.029.
[23] A. Blázquez-Moraleja, P. Moya, M.L. Marin, F. Bosca, Synthesis of novel heterogeneous photocatalysts based on Rose Bengal for effective wastewater disinfection and decontamination, Catal. Today (2022), 113948, https://doi.org/10.1016/j.cattod.2022.11.009.
[24] J. Diaz-Angulo, J.A. Lara-Ramos, F. Machuca-Martínez, Dye photosensitization on heterogeneous photocatalysis process, fundaments, and applications, in: Nanostructured Photocatalysts, Elsevier, 2021: pp. 331–362. https://doi.org/10.1016/B978–0-12–823007-7.00002-X.
[25] S. Chen, S. Chen, S. Jiang, M. Xiong, J. Luo, J. Tang, Z. Ge, Environmentally friendly antibacterial cotton textiles finished with siloxane sulfopropylbetaine, ACS Appl. Mater. Interfaces 3 (2011) 1154–1162, https://doi.org/10.1021/am101275d.
[26] W. Chen, W. Wang, X. Ge, Q. Wei, R.A. Ghiladi, Q. Wang, Photooxidation properties of photosensitizer/direct dye patterned polyester/cotton fabrics, Fibers Polym. 19 (2018) 1687–1693, https://doi.org/10.1007/s12221-018-8068-4.
[27] P. Henke, H. Kozak, A. Artemenko, P. Kubát, J. Forstová, J. Mosinger, Superhydrophilic polystyrene nanofiber materials generating O_2 ($^1\Delta_g$): postprocessing surface modifications toward efficient antibacterial effect, ACS Appl. Mater. Interfaces 6 (2014) 13007–13014, https://doi.org/10.1021/am502917w.
[28] J. Mosinger, O. Jirsák, P. Kubát, K. Lang, B. Mosinger, Bactericidal nanofabrics based on photoproduction of singlet oxygen, J. Mater. Chem. 17 (2007) 164–166, https://doi.org/10.1039/B614617A.
[29] S. Halder, K.K. Yadav, R. Sarkar, S. Mukherjee, P. Saha, S. Haldar, S. Karmakar, T. Sen, Alteration of Zeta potential and membrane permeability in bacteria: a study with cationic agents, Springerplus 4 (2015) 672, https://doi.org/10.1186/s40064-015-1476-7.
[30] Y. Nitzan, R. Dror, H. Ladan, Z. Malik, S. Kimel, V. Gottfried, Structure-activity relationship of porphines for photoinactivation of bacteria, Photochem. Photobio. 62 (1995) 342–347, https://doi.org/10.1111/j.1751-1097.1995.tb05279.x.
[31] M. Schäfer, C. Schmitz, R. Facius, G. Horneck, B. Milow, K.-H. Funken, J. Ortner, Systematic study of parameters influencing the action of Rose bengal with visible light on bacterial cells: comparison between the biological effect and singlet-oxygen production, Photochem. Photobio. 71 (2007) 514–523, https://doi.org/10.1562/0031-8655(2000)0710514SSOPIT2.0.CO2.
[32] T. Maisch, J. Baier, B. Franz, M. Maier, M. Landthaler, R.-M. Szeimies, W. Bäumler, The role of singlet oxygen and oxygen concentration in photodynamic inactivation of bacteria, Proc. Natl. Acad. Sci. 104 (2007) 7223–7228, https://doi.org/10.1073/pnas.0611328104.
[33] H.-S. Kim, E.J. Cha, H.-J. Kang, J.-H. Park, J. Lee, H.-D. Park, Antibacterial application of covalently immobilized photosensitizers on a surface, Environ. Res 172 (2019) 34–42, https://doi.org/10.1016/j.envres.2019.01.002.
[34] P. Tang, Z. Zhang, A.Y. El-Moghazy, N. Wisuthiphaet, N. Nitin, G. Sun, Daylight-induced antibacterial and antiviral cotton cloth for offensive personal protection,

ACS Appl. Mater. Interfaces 12 (2020) 49442–49451, https://doi.org/10.1021/acsami.0c15540.
[35] K. Liu, Y. Liu, Y. Yao, H. Yuan, S. Wang, Z. Wang, X. Zhang, Supramolecular photosensitizers with enhanced antibacterial efficiency, Angew. Chem. Int. Ed. 52 (2013) 8285–8289, https://doi.org/10.1002/anie.201303387.
[36] F. Jin, S. Liao, Q. Wang, H. Shen, C. Jiang, J. Zhang, Q. Wei, R.A. Ghiladi, Dual-functionalized luminescent/photodynamic composite fabrics: Synergistic antibacterial activity for self-disinfecting textiles, Appl. Surf. Sci. 587 (2022), 152737, https://doi.org/10.1016/j.apsusc.2022.152737.
[37] T. Zhang, H. Yu, J. Li, H. Song, S. Wang, Z. Zhang, S. Chen, Green light–triggered antimicrobial cotton fabric for wastewater disinfection, Mater. Today Phys. 15 (2020), 100254, https://doi.org/10.1016/j.mtphys.2020.100254.
[38] T. Wang, W. Chen, T. Dong, Z. Lv, S. Zheng, X. Cao, Q. Wei, R.A. Ghiladi, Q. Wang, Color-variable photodynamic antimicrobial wool/acrylic blended fabrics, Materials 13 (2020) 4141, https://doi.org/10.3390/ma13184141.
[39] P. Tang, A.Y. El-Moghazy, B. Ji, N. Nitin, G. Sun, Unique “posture” of Rose Bengal for fabricating personal protective equipment with enhanced daylight-induced biocidal efficiency, Mater. Adv. 2 (2021) 3569–3578, https://doi.org/10.1039/D1MA00100K.
[40] M. DeRosa, Photosensitized singlet oxygen and its applications, Coord. Chem. Rev. 233– 234 (2002) 351–371, https://doi.org/10.1016/S0010-8545(02)00034-6.
[41] J.G. Waite, A.E. Yousef, Chapter 3 Antimicrobial Properties of Hydroxyxanthenes, in: 2009: pp. 79–98. https://doi.org/10.1016/S0065–2164(09)69003–1.
[42] A.K.Roy Choudhury, Visual measures of colour, in: Principles of Colour and Appearance Measurement, Elsevier, 2015: pp. 1–25. https://doi.org/10.1533/9781782423881.1.
[43] S.-L. Jan, G. Shieh, Determining sample sizes for precise contrast analysis with heterogeneous variances, J. Educ. Behav. Stat. 39 (2014) 91–116, https://doi.org/10.3102/1076998614523069.
[44] D.R.C. and H.I.B. John W.Tukey; David R. Brillinger, The collected works of John W. Tukey, Wadsworth, 1984.
[45] H. Cramér, Mathematical methods of statistics, Princeton Univ. Pres, 1946.
[46] A. Kisner, K.T. Rainert, F. Ferrari, C.T. Nau, I.O. Barcellos, S.H. Pezzin, J. Andreaus, Chemical functionalization of polyamide 6.6 fabrics, React. Funct. Polym. 73 (2013) 1349–1356, https://doi.org/10.1016/j.reactfunctpolym.2013.03.010.
[47] B. Mu, Y. Yang, Complete separation of colorants from polymeric materials for cost-effective recycling of waste textiles, Chem. Eng. J. 427 (2022), 131570, https://doi.org/10.1016/j.cej.2021.131570.
[48] H.B. Rodríguez, M.G. Lagorio, E. San Román, Rose Bengal adsorbed on microgranular cellulose: evidence on fluorescent dimers, Photochem. Photobiol. Sci. 3 (2004) 674–680, https://doi.org/10.1039/b402484b.
[49] S. Lacombe, T. Pigot, Materials for selective photo-oxygenation vs. photocatalysis: preparation, properties and applications in environmental and health fields, Catal. Sci. Technol. 6 (2016) 1571–1592, https://doi.org/10.1039/C5CY01929J.
[50] M.A. Rauf, J.P. Graham, S.B. Bukallah, M.A.S. Al-Saedi, Solvatochromic behavior on the absorption and fluorescence spectra of Rose Bengal dye in various solvents, Spectrochim. Acta A Mol. Biomol. Spectrosc. 72 (2009) 133–137, https://doi.org/10.1016/j.saa.2008.08.018.
[51] D. Staneva, S. Yordanova, E. Vasileva-Tonkova, S. Stoyanov, I. Grabchev, Photophysical and antibacterial activity of light-activated quaternary eosin Y, Open Chem. 17 (2019) 1244–1251, https://doi.org/10.1515/chem-2019-0135.
[52] D.C. Neckers, Rose bengal, J. Photochem. Photobio. A Chem. 47 (1989) 1–29, https://doi.org/10.1016/1010-6030(89)85002-6.
[53] O. Cabezuelo, R. Martinez-Haya, N. Montes, F. Bosca, M.L. Marin, Heterogeneous riboflavin-based photocatalyst for pollutant oxidation through electron transfer processes, Appl. Catal. B 298 (2021), 120497, https://doi.org/10.1016/j.apcatb.2021.120497.
[54] C.R. Lambert, I.E. Kochevar, Electron transfer quenching of the Rose Bengal triplet state, Photochem. Photobio. 66 (1997) 15–25, https://doi.org/10.1111/j.1751-1097.1997.tb03133.x.
[55] L. Ludvíková, P. Friš, D. Heger, P. Šebej, J. Wirz, P. Klán, Photochemistry of Rose Bengal in water and acetonitrile: a comprehensive kinetic analysis, Phys. Chem. Chem. Phys. 18 (2016) 16266–16273, https://doi.org/10.1039/C6CP01710J.
[56] A. Penzkofer, M. Simmel, D. Riedl, Room temperature phosphorescence lifetime and quantum yield of erythrosine B and rose bengal in aerobic alkaline aqueous solution, J. Lumin 132 (2012) 1055–1062, https://doi.org/10.1016/j.jlumin.2011.12.030.
[57] J.C. Peterson, E. Arrieta, M. Ruggeri, J.D. Silgado, K.J. Mintz, E.H. Weisson, R. M. Leblanc, I. Kochevar, F. Manns, J.-M. Parel, Detection of singlet oxygen luminescence for experimental corneal Rose Bengal photodynamic antimicrobial therapy, Biomed. Opt. Express 12 (2021) 272, https://doi.org/10.1364/BOE.405601.
[58] M. Bregnhøj, M. Westberg, F. Jensen, P.R. Ogilby, Solvent-dependent singlet oxygen lifetimes: temperature effects implicate tunneling and charge-transfer interactions, Phys. Chem. Chem. Phys. 18 (2016) 22946–22961, https://doi.org/10.1039/C6CP01635A.
[59] E. Fuentes-Lemus, M. Mariotti, P. Hägglund, F. Leinisch, A. Fierro, E. Silva, C. López-Alarcón, M.J. Davies, Binding of Rose Bengal to lysozyme modulates photooxidation and cross-linking reactions involving tyrosine and tryptophan, Free Radic. Biol. Med 143 (2019) 375–386, https://doi.org/10.1016/j.freeradbiomed.2019.08.023.
[60] I. Berruti, M. Inmaculada Polo-López, I. Oller, J. Flores, M. Luisa Marin, F. Bosca, Sulfate radical anion: laser flash photolysis study and application in water disinfection and decontamination, Appl. Catal. B 315 (2022), 121519, https://doi.org/10.1016/j.apcatb.2022.121519.